pi -bonded N_2 on Cr(110) as a precursor for dissociation: molecular orbital theory

1992 J. Phys.: Condens. Matter 4 2429

(http://iopscience.iop.org/0953-8984/4/10/009)

J. Phys.: Condens. Matter 4 (1992) 2429–2437. Printed in the UK

π-bonded N_2 on Cr(110) as a precursor for dissociation: molecular orbital theory

Ru-Hong Zhou†‡, Dan-Hua Shi‡ and Pei-lin Cao†‡

† Centre of Theoretical Physics, CCAST (World Laboratory), PO Box 8730, Beijing 100080, People's Republic of China

‡ Department of Physics, Zhejiang University, Hangzhou 310027, People's Republic of China

Received 3 April 1991, in final form 19 July 1991

Abstract. An atom superposition and electron delocalization molecular orbital theory has been applied to the N_2 chemisorption on the Cr(110) surface in this paper. The results show that N_2 chemisorbs parallely on the fourfold site with N–N axis parallel to the [1$\bar{1}$0] direction. In contrast to the traditional σ donation and π weak-back-bonding concepts, the N_2 chemisorption on Cr(110) has both $3\sigma_g$ and $1\pi_u$ donations of 0.97 and 0.54 electrons, respectively. Meanwhile, the back-bonding to the $1\pi_g$ orbital increases to 1.83 electrons. Both these factors result in the fact that the horizontal orientation is favoured over the vertical orientation. Furthermore, the N–N bond length stretches 17%, the N–N bond order decreases to below 1, and the dissociation barrier is only about 0.15 eV. This indicates that the π-bonded α-N_2 is a precursor to the dissociation adsorption.

1. Introduction

The reaction of nitrogen and nitrogen-containing molecules with transition-metal surfaces is of considerable interest not only for technological application but also from the scientific viewpoint. It plays an important role in understanding the primary processes of the heterogeneously catalyzed ammonia synthesis. A comparison of the nitrogen chemisorption process with that of isoelectronic carbon monoxide can provide useful insight into the interactions between adsorbates and substrates. A number of experimental techniques and theoretical calculations have been applied to this field.

Both experimental [1–9] and theoretical [2, 10, 11] studies have shown that N_2 is weakly chemisorbed via one nitrogen atom and oriented with its intramolecular axis nearly perpendicular to most transition-metal surfaces, such as Ni [1–3, 10], Pd [2], Ru [4, 5], W [6, 7], Re [8] and Ir [9]. This geometry is usually described by the well known σ donation and π weak-back-bonding concepts. However, a series of recent experiments have shown that N_2 is strongly chemisorbed on Fe(111) [12, 13], Cr (111) [14] and Cr(110) [15] with its intramolecular axis parallel to the surfaces, i.e. as π-bonded α-N_2 [12]. Using the atomic superposition and electronic delocalization (ASED) molecular orbital (MO) theory, Domanek and Bennemann [16] have studied the N_2 chemisorption on Fe(111) and obtained a conclusion consistent with experiments. However, these workers have not given any explanation as to why N_2 chemisorbs parallel on Fe and perpendicular on Ni, Pd, etc. The present work is just to develop a deeper insight into

0953-8984/92/102429 + 09 $04.50

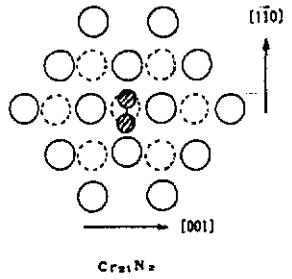

Figure 1. Cluster model $Cr_{21}N_2$ for N_2 chemisorption on the *Cr(110) surface*: ○, *first-layer Cr atom*; ◌, second-layer Cr atom; ⊘, N atom.

Table 1. The atomic parameters used in the calculations: n, principal quantum number; I_p, ionization energy; ξ, the Salter orbital exponent.

	s			p			d					
Atom	n	I_p (eV)	ξ (au)	n	I_p (eV)	ξ (au)	n	p	ξ_1 (au)	ξ_2 (au)	C_1	C_2
N	2	18.33	2.18	2	12.53	2.05						
Cr	4	8.256	1.60	4	5.374	1.30	3	9.50	4.95	1.60	0.4876	0.7205

the N_2 chemisorption on Cr(110) and further to give an explanation for the different orientations of N_2 on various transition-metal surfaces. To our knowledge this is the first theoretical study for the Cr(110)–N_2 system, and the calculation results support the experimental findings of Shinn [15] and also some new valuable results are given.

2. Models and method

In this paper, a two-layer cluster model $Cr_{21}N_2$ is employed to simulate the chemisorption and dissociation of N_2 on Cr(110) (figure 1), and the bulk nearest-neighbour distance of 2.498 Å is used. The ASED MO theory, which has been applied to the study of chemisorption on both metal and semiconductor surfaces, and has proved to be quite successful in determining the potential surfaces, bond geometries and force constants [16, 17] is adopted for the calculation. The atomic parameters are listed in table 1. With respect to the N parameters used by Domanek and Benneman [16], some small modification has been made for the N 2s orbital exponent in order to give the correct bond length of free N_2, 1.09 Å (a value of 1.15 Å was used by Domanek and Bennemann [16]), and the vibration frequency ν of 2455 cm^{-1} is only 4% larger than the experimental value of 2359 cm^{-1}. The Cr parameters are according to the treatments of Mehandru and Anderson [18] and give reasonable charge transfers and bond lengths for diatomic CrO and CrC.

3. Results and discussion

A total of eight possible chemisorption geometries are considered in our calculation: four for the vertical orientation, i.e. onefold, twofold, threefold and fourfold; four for

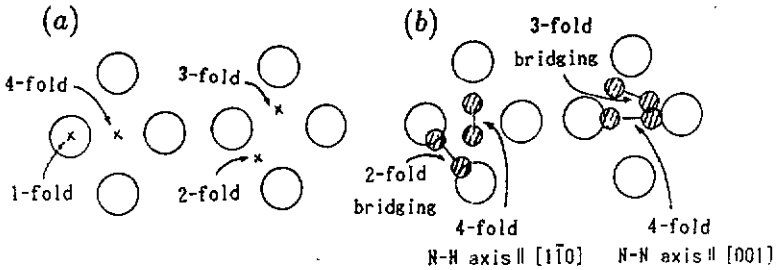

Figure 2. Eight possible adsorption geometries of N_2 on the Cr(110) surface: (*a*) vertical; (*b*) horizontal.

Table 2. Calculation results for the eight possible adsorption geometries of N_2 on Cr(110): BE, binding energy; h, adsorption height; $\Delta d_{N\text{-}N}$, stretching of the N–N bond length; Q_{N_2}, charge on the N_2 molecule; P_i $(3\sigma_g)$, P_i $(1\pi_u)$ and P_i $(1\pi_g)$, occupation numbers in the respective orbitals.

	Vertical orientation				Horizontal orientation			
	Onefold	Twofold	Threefold	Fourfold	Twofold bridging	Threefold bridging	Fourfold, N–N∥[001]	Fourfold, N–N∥[1$\bar{1}$0]
BE (eV)	4.17	4.01	3.79	3.11	5.77	6.02	5.52	6.34
h (Å)	1.52	1.24	1.14	1.10	1.32	1.06	1.30	0.92
$\Delta d_{N\text{-}N}$ (Å)	0.06	0.05	0.05	0.04	0.14	0.16	0.10	0.19
Q_{N_2}	−0.5	−0.59	−0.65	−0.58	−0.48	−0.48	−0.42	−0.32
$P_i(3\sigma_g)$	1.45	1.51	1.63	1.65	1.49	1.45	1.41	1.03
$P_i(1\pi_u)$	4.0	4.0	4.0	4.0	3.70	3.62	3.80	3.46
$P_i(1\pi_g)$	1.05	1.08	1.12	0.93	1.29	1.41	1.21	1.83

the horizontal orientation, i.e. twofold bridging, threefold bridging, fourfold with N–N axis parallel to [001], and fourfold with N–N axis parallel to [1$\bar{1}$0] (figure 2). For each chemisorption geometry we have calculated the curves of the total energy versus the adsorption height h (defined as the vertical distance of the nearer N atom from the substrate for the vertical orientation, and the length of the N–N bond for the horizontal orientation) and the N_2 bond length $d_{N\text{-}N}$. From the minimization of the total energy we can obtain the optimized adsorption heights, N–N bond lengths, binding energies and charge transfers. The calculated results are listed in table 2. It is obvious that all the horizontal orientations are favoured over all the vertical orientations. The fourfold site with N–N axis parallel to the [1$\bar{1}$0] direction is the most stable geometry, and its bonding energy is 2.17 eV larger than that of the onefold vertical orientation. This result confirms the experimental findings of Shinn [15] who proposed a π-bonded α-N_2 on Cr(110), but Shinn did not give an accurate chemisorption geometry. From figure 2, we can see that our result is reasonable because the fourfold site with the N–N axis parallel to [1$\bar{1}$0] uniquely allows each N atom to bind to three surface Cr atoms, accounting for its stability; this is also analogous to the chemisorption of CO on Cr(110) [18].

In order to examine the dependence of the calculation to the size and structure of the Cr cluster, we studied another two clusters, Cr_5N_2 (four atoms in the first layer, and

Table 3. Comparison of the calculation results of the three cluster models for the fourfold site with the N–N axis parallel to [1$\bar{1}$0]. The symbols have the same meanings as those in table 2.

Cluster	BE (eV)	h (Å)	Δd_{N-N} (Å)	Q_{N_2}	$P_i(3\sigma_g)$	$P_i(1\pi_u)$	$P_i(1\pi_g)$
Cr_5N_2	6.10	0.88	0.23	−0.38	1.28	3.18	1.92
$Cr_{21}N_2$	6.34	0.92	0.19	−0.32	1.03	3.46	1.83
$Cr_{33}N_2$	7.08	0.92	0.18	−0.34	1.09	3.40	1.85

Table 4. Binding energies of the three cluster models for the eight possible geometries.

	BE (eV)							
Cluster	Onefold	Twofold	Threefold	Fourfold	Twofold bridging	Threefold bridging	Fourfold, N–N‖[001]	Fourfold, N–N‖[1$\bar{1}$0]
Cr_5N_2	4.02	3.90	3.45	3.20	5.50	5.75	5.28	6.10
$Cr_{21}N_2$	4.17	4.01	3.79	3.11	5.77	6.02	5.52	6.34
$Cr_{33}N_2$	4.36	4.33	3.83	3.40	6.56	6.78	6.40	7.08

one atom in the second layer) and $Cr_{33}N_2$ (18 atoms in the first layer, 11 atoms in the second layer and four atoms in the third layer). Table 3 lists the calculation results of the three clusters for the adsorption geometry of the fourfold site with N–N axis parallel to [1$\bar{1}$0]. The results show that the adsorption heights, N–N bond lengths, charge transfers and molecular orbital occupation numbers are very close for the three clusters, especially for $Cr_{21}N_2$ and $Cr_{33}N_2$. Similar calculations for the other seven geometries also result in the same conclusion. Only the binding energy changes in some degree with the cluster size (the reason for this is under further investigation), as listed in table 4. From table 4, we can see that the geometry of the fourfold site with the N–N axis parallel to [1$\bar{1}$0] is the most stable in all the three cluster models, and the differences between the binding energies of the adsorption geometries are nearly equal for the three clusters. All the above results indicate that our calculation for the bond geometry using the cluster $Cr_{21}N_2$ should be reliable. In fact, at present, the cluster models in the molecular orbital theories usually contain 10–30 atoms for calculation [16–20]. So we adopted $Cr_{21}N_2$ cluster in the following study.

The translation behaviours of the N_2 molecule on the Cr(100) surface are investigated in this paragraph. Three kinds of translation are contained in our calculation:

(i) moving between vertical orientations;
(ii) moving between horizontal orientations;
(iii) changing from a vertical orientation to a horizontal orientation.

Figure 3 shows three typical examples for the three kinds of translation:

(a) Onefold → twofold → onefold;
(b) fourfold with the N–N axis parallel to [1$\bar{1}$0] → twofold bridging → fourfold with the N–N axis parallel to [1$\bar{1}$0];
(c) vertical → horizontal on a fourfold site.

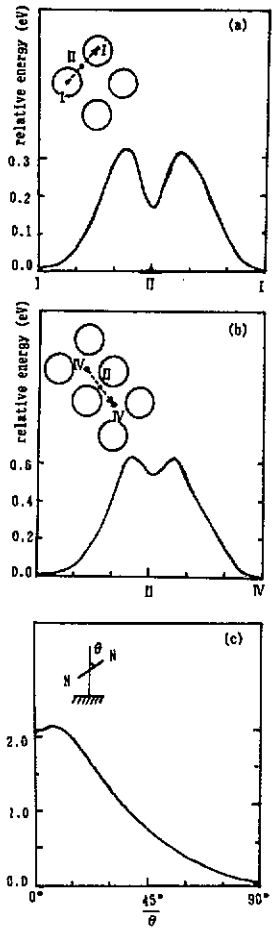

Figure 3. Translation between adsorption geometries: (*a*) onefold → twofold → onefold (vertical orientation); (*b*) fourfold (N–N axis∥[1$\bar{1}$0]) → twofold briding → fourfold (N–N axis∥[1$\bar{1}$0]) (horizontal orientation); (*c*) vertical → horizontal orientation on the fourfold site.

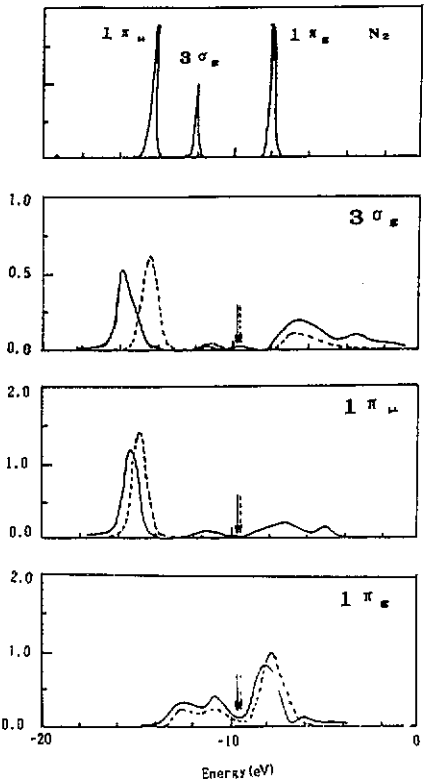

Figure 4. The LDOSs of N_2 $3\sigma_g$, $1\pi_u$ and $1\pi_g$ orbitals: ——, LDOS on fourfold site (N–N axis parallel to [1$\bar{1}$0]); – – –, LDOS on a onefold site (N_2 vertical). The position of the Fermi energy is indicated by an arrow.

The potential barriers for the three cases (a), (b) and (c) are found to be 0.32 eV, 0.65 eV and 0.05 eV, respectively (the N–N bond length and orientation have been optimized in translation paths). The small barrier for the vertical to horizontal orientation indicates that horizontal orientations are strongly favoured. Since other translations and jumps show similar behaviours, we omit detailed analyses here.

As the fourfold vertical orientation and the fourfold with the N–N axis parallel to [001] are both unfavoured geometries, we simply name the fourfold with the N–N axis parallel to [1$\bar{1}$0] as the fourfold site in the following, and the onefold vertical orientation simply as the onefold site.

Then, why does the N_2 chemisorption on Cr(110) appear as a horizontal orientation different from the other transition-metal surfaces, such as Ni and Pd? We attempt to

give some explanation for this by analysing the electronic structures. Anderson and co-workers [18, 19] have reported that carbon monoxide adsorbs in a vertical orientation on the metals on the right-hand side of the transition series, e.g. Ni, Pt, Pd and Cu, and favours a horizontal orientation on the left-hand side, e.g. Cr. They have also suggested that the horizontal orientation is a result of the destabilization and emptying of the antibonding counterparts to CO 5σ and 1π donation bonds on the Cr surface and that the back-bonding to CO 2π orbitals is enhanced when horizontal. Here, we have given a more detailed discussion and proposed that the main factor in determining the adsorption orientations of N_2 or CO on metal may not be simply the left- or right-hand sides in the transition-metal series but the number of d orbital electrons and the relative Fermi energy levels, because experiments have found that N_2 adsorbs perpendicularly on W(100) and [6, 7] surfaces, although W is also on the left-hand side of the transition-metal series and actually in the same vertical group as Cr (we are investigating this further by studying the N_2–W system).

In order to have a clear picture of this, we turn to study the local density of states (LDOS) for the N_2 molecular orbitals $3\sigma_g$, $1\pi_u$ and $1\pi_g$. The following equation has been used in the calculation of the LDOS [20, 21]:

$$d_i(E) = \sum_k |\langle \psi_i | \varphi_k \rangle|^2 \, \delta(E - E_k) = \sum_k |\langle \psi_i | \varphi_k \rangle|^2 \frac{\sigma/\pi}{(E_k - E)^2 + \sigma^2}$$

where ψ_i is the molecular orbital of free N_2, e.g. $3\sigma_g$, $1\pi_u$, $1\pi_g$, φ_k is the kth molecular orbital of the system Cr_2N_2 and σ is the Lorentzian-broadened width which is 0.25 eV. The orbital populations P_i are given by

$$P_i = \int_{-\infty}^{E_F} d_i(E) \, dE.$$

They are also collected in table 2. Figure 4 shows the LDOSs of $3\sigma_g$, $1\pi_u$ and $1\pi_g$ orbitals on the fourfold and onefold sites. From figure 3, we can find that both the bonding orbitals $3\sigma_g$ and $1\pi_u$ and the antibonding orbital $1\pi_g$ of the free N_2 are contained in the binding with the substrate. Furthermore, with respect to the onefold site, the fourfold site has not only $3\sigma_g$ but also $1\pi_u$ donation bonds. That is to say, when horizontal, both $3\sigma_g$ and $1\pi_u$ orbitals are split into the bonding counterparts $3\bar{\sigma}_g$ and $1\bar{\pi}_u$ and the antibonding counterparts, owing to the interaction of the substrate. The bonding parts $3\bar{\sigma}_g$ and $1\bar{\pi}_u$ are going to have larger binding energies than that of the onefold vertical orientation, while the antibonding counterparts are high lying, just above the Cr 3d band and also above the Fermi energy, and empty. On the other hand, the population numbers of $3\sigma_g$, $1\pi_u$ and $1\pi_g$ orbitals (see table 2) also suggest that in the vertical orientations the $1\pi_u$ orbital is filled, while in the horizontal orientations it donates 0.20–0.54 electrons. For the fourfold site, the $3\sigma_g$ and $1\pi_u$ donations are as large as 0.97 and 0.54 electrons, respectively, which means that the empty antibonding counterparts of $3\sigma_g$ and $1\pi_u$ orbitals are 49% and 14%, respectively. The empty antibonding counterparts and the more stable bonding parts of $3\sigma_g$ and $1\pi_u$ make the horizontal orientation favoured over the vertical orientation. Meanwhile, the back-bonding to the $1\pi_g$ orbital is also enhanced when horizontal, increasing from 26% for the onefold site to 46% for the fourfold site. Both these factors result in the fact that the horizontal orientation is favoured for N_2 on Cr(110) and it is a strong chemisorption.

While, for the N_2 chemisorption on Ni surfaces [2, 10], there are more Ni 3d electrons and the Fermi energy is higher, which means that the antibonding counterparts of $3\sigma_g$

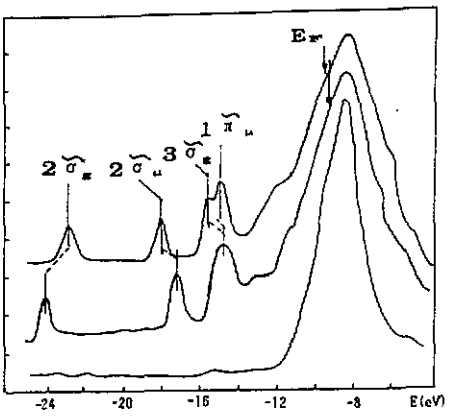

Figure 5. The TDOSs for the system: curve A, Cr_{21}; curve B, $Cr_{21}N_2$, N_2 on a onefold site, vertical; curve C, $Cr_{21}N_2$, N_2 on a fourfold site, N–N axis parallel to $[1\bar{1}0]$.

and $1\pi_u$ orbitals are mostly below the Fermi energy and filled. Then the orientation of N_2 is influenced by the Ni 3d electrons and the vertical orientation is now favoured in order to avoid a strong closed-shell repulsion [18]. In our previous DV–X_α calculation [10] for N_2 on Ni surfaces, the $1\pi_u$ orbital is filled, the $3\sigma_g$ donation is 0.17 electrons, and the $1\pi_g$ back-donation is 0.48 electrons. Compared with the N_2–Cr(110) system, it is clearly a weak chemisorption, also confirmed by experiments [1–3]. So we can predict that, from Cr to Ni, with the increase in d electrons, the occupation of the $3\sigma_g$ and $1\pi_u$ antibonding counterparts also increases gradually, which reduces the stability gained owing to the donation bonds and results in a change in the chemisorption geometry from the horizontal orientation to the vertical orientation.

In order to make a direct comparison with Shinn's [15] UPS spectrum, we also calculated the total density of states (TDOS) for the system:

$$D(E) = \sum_k \delta(E - E_k) = \sum_k \frac{\sigma/\pi}{(E - E_k)^2 + \sigma^2}.$$

The TDOSs of Cr_{21}, $Cr_{21}N_2$ with N_2 on a fourfold site, and $Cr_{21}N_2$ with N_2 on a onefold site are shown in figure 5. For the vertical orientation, the $3\tilde{\sigma}_g$ and $1\tilde{\pi}_u$ peaks are mixed while, for the horizontal orientation, $3\tilde{\sigma}_g$ and $1\tilde{\pi}_u$ are split into two peaks and in particular the $3\tilde{\sigma}_g$ peak moves 0.4 eV below the $1\tilde{\pi}_u$ in agreement with the UPS experiment (the $2\tilde{\sigma}_u$, $3\tilde{\sigma}_g$ and $1\tilde{\pi}_u$ peaks are 12.7 eV, 8.4 eV and 7.1 eV, respectively, below E_F [15]). Thus, the TDOS calculation also confirms the conclusion of the N_2 horizontal orientation. However, the present results for the energy levels of $2\tilde{\sigma}_u$, $3\tilde{\sigma}_g$ and $1\tilde{\pi}_u$, and their splitting distances are somewhat different from the experimental values, which may be due to the neglect of the screening effect of the final state in the ASED method [21].

From table 2, one can find that on a fourfold site (N–N axis parallel to [110]) the N–N bond length has stretched 17%, being 1.28 Å, which indicates a very large decrease in the N–N stretching frequency. Fukuda and Nagosgi [14], using high-resolution electron energy loss spectroscopy (HREELS), have studied the chemisorption of N_2 on Cr(111) and found a vibrational frequency of 1170 cm^{-1}, which is almost half that on Ni(100) [2], Ru(100) [5] and W(100) [7] (around 2200 cm^{-1}). Here we employed a crude approximation by omitting the N_2 vibrational coupling to the surface and used an elementary formula for the force constants, $ke = (\Delta^2 E/\Delta R^2)e$. Then, the vibrational frequency is obtained: $\nu = 1050\ cm^{-1}$, which is still 10% lower than that on Cr(111) (this needs to be

Table 5. Adsorption of N atom on Cr(110): BE, binding energy; h, adsorption height.

Site	Onefold	Twofold	Threefold	Fourfold
BE (eV)	4.81	4.40	4.51	3.56
h (Å)	1.46	0.94	0.80	0.80

confirmed by a HREELS experiment). According to the viewpoint of Tsai *et al* [22], the N–N stretching frequency of compounds containing N_2 decreases from 2359 cm^{-1} for gaseous N_2, to 1570–1440 cm^{-1} for those compounds with an N–N bond order of 2, and to about 1100 cm^{-1} for those compounds with an N–N bond order of 1. On the other hand, the N–N bond length increases from 1.09 Å to 1.23 Å to 1.25 Å when the N–N bond order decreases from 3 to 2 to 1, respectively. So we can say that, when N_2 chemisorbs on the Cr(110) surface, the strong $3\sigma_g$ and $1\pi_u$ donations and $1\pi_g$ back-donation both serve to weaken the N–N bond extremely, and the bond order decreases to below 1. The vibrational stretching frequency of N_2 on Fe(111) is 1490 cm^{-1} [12], 27% larger than that on Cr(111), which implies stronger $3\sigma_g$ and $1\pi_u$ donations and $1\pi_g$ back-donation on Cr(111) than that on Fe(111), consistent with the former analysis.

The lower N–N stretching frequency on Cr(110) also indicates an easier dissociation process than that on Fe(111), where the dissociation barrier is 0.4 eV [16]. A detailed calculation has been performed for the dissociation process. The results show that there is a barrier of 0.15 eV in the dissociation path on the fourfold site, and similar calculations for the dissociation on twofold bridging and threefold bridging sites also show a barrier of 0.2 ± 0.05 eV. This low barrier is in good agreement with the observed low temperature (100 K or below) dissociation [15] and also indicates that the π-bonded N_2 is a precursor state to N_2 dissociation. The adsorption states for the dissociated N atoms are collected in table 5. We can see that the dissociated N atoms will finally adsorb on the onefold sites, with a binding energy of 4.81 eV. That is to say, when a N_2 molecule dissociates into two N atoms, it will release an energy of 3.28 eV.

4. Conclusions

N_2 chemisorbs parallel on the fourfold site on Cr(110) surface with the N–N axis parallel to the $[1\bar{1}0]$ direction, and the adsorption height is 0.92 Å.

In contrast to the traditional σ donation and π weak-back-bonding concepts, the N_2 chemisorption on Cr(110) has both $3\sigma_g$ and $1\pi_u$ donations of 0.97 and 0.54 electrons, respectively. Meanwhile, the back-bonding to the $1\pi_g$ orbital increases to 1.83 electrons. Both these factors result in the fact that the horizontal orientation favoured over the vertical orientation.

In the TDOS for $Cr_{21}N_2$ (N_2 on the fourfold site with the N–N axis parallel to $[1\bar{1}0]$), $3\bar{\sigma}_g$ and $1\bar{\pi}_u$ are split into two peaks, and in particular $3\bar{\sigma}_g$ moves to below $1\bar{\pi}_u$. This supports Shinn's UPS results.

The N–N bond length has stretched 17%; the stretching vibrational frequency decreases to 1050 cm^{-1}. According to the viewpoint of Tsai *et al*, the N–N bond order decreases to below 1. The dissociation barrier is only 0.15 eV. This indicates that the π-bonded α-N_2 is a precursor to N_2 dissociation.

References

[1] Bagus P S, Brundle C R, Hermann K and Menzel D 1980 *J. Electron Spectrosc. Relat. Phenom.* **20** 253
[2] Horn K, Dinardo J, Eberhardt W, Freund H-J and Plummer E-W 1982 *Surf. Sci.* **118** 465
[3] Dowben P A, Sakisaka Y and Rhodin T N 1984 *Surf. Sci.* **147** 89
[4] Heskett D, Plummer E W, Depaola R A, Eberhardt W, Hoffmann F M and Moser H R 1985 *Surf. Sci.* **164** 490
[5] Depaola R A and Hoffmann F M 1986 *Chem. Phys. Lett.* **128** 343
[6] Umbach E 1984 *Solid State Commun.* **51** 365
[7] Ho W, Willis R F and Plummer E W 1980 *Surf. Sci.* **95** 171
[8] Hasse G and Asscher M 1987 *Surf. Sci.* **191** 75
[9] Ibbotson D E, Wittrig T S and Weinberg W H 1981 *Surf. Sci.* **110** 313
[10] Wu Yue and Cao Pei-Lin 1987 *Surf. Sci.* **179** L26
[11] Heskett D, Plummer E W and Messmer R P 1984 *Surf. Sci.* **139** 558
[12] Grunze M, Golze M, Hirschwald W, Freund H-J, Pulm H, Seip U, Tsai M C, Ertl G and Küppers J 1984 *Phys. Rev. Lett.* **53** 850
[13] Freund H-J, Bartos B, Messmer R P, Grunze M, Kuhlenbeck H and Neumann M 1987 *Surf. Sci.* **185** 187
[14] Fukuda Y and Nagosgi M 1988 *Surf. Sci.* **203** L651
[15] Shinn N D 1990 *Phys. Rev.* B **41** 9771
[16] Tomanek D and Bennemann K H 1985 *Phys. Rev.* B **31** 2488
[17] Cao Pei-Lin and Zhang Zhong-Guo 1989 *Phys. Rev.* B **39** 9963
Zhou Ru-Hong and Cao Pei-Lin 1991 *Surf. Sci.* **243** L49
[18] Mehandru S P and Anderson A B 1986 *Surf. Sci.* **169** L281
[19] Anderson A B and Onwood D P 1985 *Surf. Sci.* **154** L261
[20] Cao Pei-Lin, Ellis D E and Freeman A J 1982 *Phys. Rev.* B **25** 2124
[21] van Langeveld A D, de Koster A and van Santen R A 1990 *Surf. Sci.* **225** 143
[22] Tsai M-C, Seip U, Bassignana I C, Küppers J and Ertl G 1985 *Surf. Sci.* **155** 387